Published in final edited form as:
Brain Struct Funct. 2009 October ; 213(6): 571. doi:10.1007/s00429-009-0218-4.

Measurement of Spontaneous Signal Fluctuations in fMRI: Adult Age Differences in Intrinsic Functional Connectivity

Nan-kuei Chen[1], **Ying-hui Chou**[2], **Allen W. Song**[1], and **David J. Madden**[1,3]

[1]Brain Imaging and Analysis Center, Duke University Medical Center, Durham NC 27710 USA

[2]Department of Occupational Therapy, Fu Jen Catholic University, Taiwan

[3]Center for the Study of Aging and Human Development, Duke University Medical Center, Durham NC 27710 USA

Abstract

Functional connectivity (FC) reflects the coherence of spontaneous, low-frequency fluctuations in functional magnetic resonance imaging (fMRI) data. We report a behavior-based connectivity analysis (BBCA) method, in which whole-brain data are used to identify behaviorally-relevant, intrinsic FC networks. Nineteen younger adults (20-28 years) and 19 healthy, older adults (63-78 years) were assessed with fMRI and diffusion tensor imaging (DTI). Results indicated that FC involving a distributed network of brain regions, particularly the inferior frontal gyri, exhibited age-related change in the correlation with perceptual-motor speed (choice reaction time; RT). No relation between FC and RT was evident for younger adults, whereas older adults exhibited a significant age-related slowing of perceptual-motor speed, which was mediated by decreasing FC. Older adults' FC values were in turn associated positively with white matter integrity (from DTI) within the genu of the corpus callosum. The developed FC analysis illustrates the value of identifying connectivity by combining structural, functional, and behavioral data.

Keywords

Aging; Brain imaging; Functional connectivity; Cognition; White matter integrity; Reaction time

Introduction

Neuroimaging research on age-related changes in brain function has focused nearly exclusively on task-related activation (Dennis & Cabeza 2008, Grady 2008). Several forms of evidence, however, suggest that decreases in brain activity (i.e., deactivation) are also informative measures. Research with younger adults has demonstrated that the level of the blood oxygen level-dependent (BOLD) signal during functional magnetic resonance imaging (fMRI) is lower, in some brain regions, during a cognitive task than during a resting or baseline condition. In particular, medial cortical regions including the posterior cingulate and medial prefrontal cortex exhibit significantly decreased brain activity during task conditions (Shulman et al. 1997, Binder et al. 1999, Mazoyer et al. 2001). Raichle et al. (2001) proposed that these posterior cingulate and medial prefrontal regions form the nodes of a *default mode network* that is continuously and spontaneously active, even in the absence of an external task. It is this

Address correspondence to: David J. Madden, Box 2980, Duke University Medical Center Durham, NC 27710, Ph: (919) 660-7537, Fax: (919) 668-0453 djm@geri.duke.edu.

spontaneous activity within the default mode network that must be suppressed during externally-directed cognitive tasks and is expressed as task-related deactivation.

Further investigations of this default mode network have demonstrated that the regions comprising the network exhibit *functional connectivity* (FC), that is, a temporal coherence of activity in the low frequency (< 0.1 Hz) component of the BOLD signal. Typically, when fMRI scanning is conducted concurrently with a cognitive task, the spontaneous, low-frequency fluctuations in the BOLD signal are considered noise and are removed in post-processing. These signal components, however, although not attributable to specific task or external stimuli, contain valuable information regarding brain activity. Greicius et al. (2003) were the first to report that spontaneous, low-frequency activity is correlated across the medial prefrontal and posterior cingulate regions, indicative of intrinsic FC in the default mode network (Fox et al. 2005). Functional connectivity studies based on spontaneous signal fluctuations are frequently performed during a continuous resting state. But spontaneous BOLD signal fluctuations can also be measured from off-task periods in block-design fMRI, as well as from event-related fMRI after suppressing the task evoked signal changes (Fair et al. 2007), enabling mapping of intrinsic FC from non-resting-state fMRI data. Evidence from combined fMRI and diffusion tensor imaging (DTI) suggests that resting state FC within the default mode network reflects the structural connectivity of associated white matter pathways (van den Heuvel et al. 2008, Greicius et al. 2009).

Several other intrinsic connectivity networks have also been identified, based on the spatial coherence of spontaneous BOLD signals, which involve several cortical regions outside of those typically associated with the default mode network. These networks appear to represent activity within neural systems mediating attention (Fox et al. 2006), motor control (Biswal et al. 1995, Xiong et al. 1999, Fox et al. 2007), language (Hampson et al. 2002), and other cognitive abilities (Damoiseaux et al. 2006, De Luca et al. 2006). Variation in these FC networks is associated closely with aspects of behavioral performance. Fox et al. (2007), for example, reported that 74% of the variability of the BOLD response in the left sensorimotor cortex, associated with the force of a right button-press, was also shared with intrinsic, spontaneous activity within the right sensorimotor cortex. Seeley et al. (2007) found that intrinsic FC in separate cortical networks, mediating executive control and the detection of salient stimuli, respectively, were dissociable and exhibited different patterns of correlation to behavioral performance.

Age-Related Changes in Default Mode Network Activity

Changes in the functioning of the default mode network have been reported for healthy older adults, relative to younger adults, in several studies of the mean level of activation. Overall, these studies suggest that older adults exhibit increased difficulty in suppressing the spontaneous signal fluctuations, within the default mode network, thus possibly reducing attentional allocation to task-relevant processing (Lustig et al. 2003, Persson et al. 2007). Investigations of the temporal coherence of low-frequency, spontaneous fluctuations in the BOLD signal (i.e., intrinsic FC) have demonstrated age-related change that is consistent with the studies of deactivation. Across several investigations, FC in the default mode network has been found to be lower for healthy older adults than for younger adults (Andrews-Hanna et al. 2007, Wu et al. 2007, Damoiseaux et al. 2008, Sambataro et al. 2008), with further decline evident in early-stage Alzheimer's disease (Greicius et al. 2004). Thus, older adults exhibit both less ability to suppress default mode activity and less FC within the network. The decreased connectivity, in turn, is associated with decreased performance in some cognitive tasks, including motor control (Wu et al. 2007), executive functioning (Andrews-Hanna et al. 2007, Damoiseaux et al. 2008), memory (Andrews-Hanna et al. 2007, Sambataro et al. 2008), and perceptual speed (Andrews-Hanna et al. 2007).

The conventional seed-based and independent components analysis (ICA)-based characterization of FC, used in previous FC studies, are illustrated in Figure 1. In the seed-based analysis (Figure 1, panel A), the time course of the BOLD signal change is correlated, on a voxelwise basis throughout the brain, with the time course of a seed ROI, and a functional network is identified from this set of correlation coefficients (Biswal et al. 1995). This approach is appropriate when sufficient *a priori* information is available to define the seed region.

In the ICA-based analysis (Figure 1, panel B), multiple functional networks (i.e., the ICA components) can be identified without prior selection of ROIs (Damoiseaux et al. 2006). The identified networks are usually sorted, in a descending order, based on the degree of signal coherence within each ICA component. The ICA-based approach enables identification of networks with a high degree of within-network signal coherence (e.g., the default mode network in younger adults), and the relation between the networks and behavioral performance can be assessed.

In previous fMRI studies of intrinsic functional connectivity related to aging, the main focus has primarily been on detecting differences in the functional connectivity strength between younger and older adults. As a result, the correlation between the connectivity strength and behavioral performance has been measured only for those networks with different connectivity levels between younger and older participants (as illustrated in Figure 1: Panels B and C). In contrast, here we report a whole-brain behavior-based connectivity analysis (BBCA) method to identify the functional connectivity networks that are best correlated with the behavioral measures, independently of the connectivity level difference between age groups.

One may use the following analogy to easily conceptualize the difference between the conventional approach and the new BBCA method. In the conventional approach, the first step would be to demonstrate a reliable difference between two data sets. For example, in evaluating the differences in food consumption between two species of animals (e.g., rats and rabbits), the average difference in body weight would first be established. If the body weights of two species differ significantly, then the body weight would be further correlated with the food consumption between species. In the BBCA approach, in contrast, the goal would be to evaluate whether the dependence of body weight on food consumption differs between the two species, regardless of the average weight. Even if the body weights of two species are similar (e.g., rats and birds), it is possible that the body weight is highly correlated with the food consumption only in one species, but not on the other. Obviously, these two approaches provide different types of information regarding the studied biological system. Therefore, the BBCA methodology will provide information that is complementary to that obtained with conventional resting-state fMRI analysis methods.

As illustrated in Figure 1 (panel C), in the BBCA method the whole-brain functional connectivity analyses are first performed, for each participant, on fMRI data with event-related responses suppressed. Then, within the matrix representing the functional connectivity between every pair of anatomical regions, each connectivity value (Fisher r to Z transform) is then correlated with behavioral data, across participants. In this approach, a behaviorally-relevant FC network is defined by a set of anatomical region pairs (matrix cells) exhibiting a high correlation with the behavioral measure.

In conventional single-subject fMRI analyses, the fMRI time course profiles are usually analyzed against the concurrently acquired behavioral-data time course profiles (e.g., in event-related fMRI) or the task-paradigm time course profiles, or without a prior model (e.g., in ICA). In contrast to conventional approaches, the developed BBCA method is based on a completely different strategy, identifying the behaviorally-relevant connectivity networks by correlating fMRI data and a single behavioral measures from multiple subjects (Figure 1C). Using this

strategy, the BBCA method is even capable of identifying connectivity networks associated with non-dynamic clinical measures or neuropsychological data that are obtained outside the MRI scanner. This type of behavior-based multi-subject imaging data analysis has been previously used in structural MRI and DTI, in which voxel-wise statistics are carried out to find areas which correlate to the covariate of interest, such as a disability score (e.g., Smith et al. 2006). However, to our knowledge, the application of behavior-based multi-subject imaging data analysis to mapping functional connectivity networks has not yet been pursued.

The goal of the present study was to use the BBCA method to discriminate the pattern of behaviorally-relevant, intrinsic FC networks of healthy younger and older adults. In view of the fundamental role of perceptual-motor speed in multiple forms of age-related cognitive change (Salthouse 1996, Madden 2001, Salthouse & Madden 2007), we used choice reaction time (RT) as the behavioral measure of primary interest. Although these analyses were largely exploratory, three hypotheses were particularly relevant. First, because voxelwise methods such as ICA typically can yield 5-10 spatially independent FC patterns (Damoiseaux et al. 2006, De Luca et al. 2006), we predicted that our method would detect FC outside of the brain regions (e.g., medial prefrontal and posterior cingulate cortex) that typically define the default mode network. Second, in view of previous reports that normal aging is associated with a decline in FC of the default mode network (Andrews-Hanna et al. 2007, Damoiseaux et al. 2008, Sambataro et al. 2008), we hypothesized that behaviorally-relevant FC outside of the default mode network would differ between younger and older adults. Third, we hypothesized that individual differences in cerebral white matter integrity, as estimated from DTI, would be associated with variation in behaviorally-relevant, intrinsic FC. This hypothesis is based on recent evidence that intrinsic FC is constrained by structural connectivity of white matter pathways (Andrews-Hanna et al. 2007, van den Heuvel et al. 2008, Greicius et al. 2009).

Materials and Methods

Participants

Participants were 19 younger adults (nine men) between 20 and 28 years of age (mean = 23.89) and 19 older adults (nine men) between 63 and 78 years of age (mean = 69.59). Results from analyses of the DTI and behavioral data have been reported previously (Bucur et al. 2008). Procedures were approved by the Institutional Review Board of the Duke University Medical Center, and all participants gave written informed. All participants were right-handed, community-dwelling individuals. On a screening questionnaire (Christensen et al. 1992), all participants reported being free of significant health problems such as atherosclerotic cardiovascular disease or hypertension, and that they were not taking medications known to significantly affect cognitive functioning or cerebral blood flow. Participants scored a minimum of 27 points on the Mini Mental State Exam (Folstein et al. 1975), a maximum of 9 on the Beck Depression Inventory (Beck 1978), and had a minimum corrected binocular acuity for near point of 20/40. Each participant's T_2-weighted structural brain images were reviewed by a neuroradiologist and judged to be within normal limits. All participants had completed at least 12 years of education; the raw scores on the vocabulary subtest of the Wechsler Adult Intelligence Scale-Revised (Wechsler 1981) did not differ significantly between the age groups (younger adults' mean = 64.63; older adults' mean = 66.68). Elementary perceptual speed, as assessed by reaction time (RT) per item on a computerized digit-symbol test, was slower for older adults (mean = 1770 ms) than for younger adults (mean = 1283 ms), $t(36) = 5.34$, $p < .01$.

Participants completed the psychometric and screening tests in a separate session ~ 2 weeks before the scanning session. During the screening session participants also performed brief versions of the behavioral tasks.

Behavioral Tasks

During scanning, participants performed three types of behavioral tasks: choice RT, episodic memory, and semantic memory. The tasks were created using Matlab (Mathworks, Natick, MA) Psychophysics Toolbox extensions (Brainard 1997). The stimuli for the memory tasks were 312 concrete nouns 4-9 letters long (mean = 6), with a Kučera-Francis (1967) word frequency of 10-849 (median = 25). Words were selected to be unambiguously classified as living (e.g., *rabbit*) or as nonliving (e.g., *mirror*), respectively, and each category comprised 156 words. A different set of 72 words, with similar properties, were used in the practice task. During scanning, participants viewed the displays with liquid-crystal display goggles (Resonance Technology, Northridge, CA), which were equipped with removable lenses, as necessary, to match the distance component of the participant's prescription. The stimulus words always appeared centrally, in white lowercase 56-point Arial font on a black background. Responses during scanning were collected from a four-button fiber optic response box (Resonance Technology). Participants rested one finger of each hand on the far left and the far right response buttons throughout the scanning session.

The behavioral tests were performed during four fMRI runs, illustrated in Figure 2. Prior to each run, participants performed a study (encoding) phase for the memory tasks, in which they viewed a series of 39 words (presented one at a time for 3 s each) and made a pleasant/unpleasant judgment regarding each word as it appeared, using the left and right response buttons. Diffusion tensor imaging was conducted during the encoding task. Each functional run (6 min, immediately following the encoding task) included, in this order: a choice RT task, an off-task interval, and a memory retrieval task. In the choice RT task, participants viewed a series 30 displays (1.5 s each) and pressed either the left or right response button at the onset of each display. Each display was followed by a jittered, ITI of either 1000, 1500, or 2000 ms. In one type of choice RT task, these displays were the words *left* and *right*, and in another type they were single arrows pointing to one of the response buttons. The choice RT task began with a 3 s instruction screen, and the word/arrow versions of the task were alternated across the four functional runs. This task was followed by a 30 s off-task period, in which a single fixation cross was in view. The choice RT task and the off-task period served as a retention interval for the 39 words studied during the encoding task.

Following the off-task period, a 3 s instruction screen appeared, which indicated whether the upcoming retrieval task was episodic or semantic. There were 78 test words (1.5 s each, plus jittered ITI) during the retrieval interval. For episodic retrieval, participants used the two response buttons to indicate whether each word was a member of the recently studied list (i.e., *old* or *new*). For semantic retrieval, the two responses represented whether the current word referred to a *living* or *nonliving* object (i.e., natural/artificial), regardless of whether the word had occurred in the study list. For each type of memory retrieval, the two response categories were represented equally. Individual words occurred only once per study/retrieval list, and items were counterbalanced across participants for occurrence in the episodic/semantic retrieval conditions. Each participant performed the semantic and episodic retrieval tests in one of two orders (ABBA or BAAB), which was counterbalanced across participants. At the beginning of the scanner session, participants completed (during structural imaging) practice versions of the choice RT and memory retrieval tasks.

Imaging Data Acquisition

Scanning was conducted on a 4T GE scanner (GE Healthcare, Waukesha, WI). A vacuum-pack system molded to each participant's head was used to minimize head motion. Participants wore earplugs to reduce the scanner noise. Anatomical scanning started with nine T_1-weighted sagittal localizer images, spanning the midline. High-resolution T_1 images were acquired with a 3D fast inverse-recovery-prepared SPGR sequence with 60 contiguous oblique slices, parallel

to the plane connecting the anterior and posterior commissures (AC-PC), TR/TE = 500/5.4 ms, number of excitations (NEX) = 1, in-plane resolution = 0.94 mm^2, field of view (FOV) = 24 cm, and slice thickness = 1.9 mm.

Functional T_2*-weighted images sensitive to BOLD contrast were acquired within the same slice prescription as the T_1-weighted images, with 30 contiguous slices parallel to the AC-PC plane. The functional scans used an inverse-spiral imaging sequence, TR/TE = 1500/31 ms, NEX = 1, in-plane resolution = 3.75 mm^2, flip angle = 80°, FOV = 24 cm, image matrix = 64 × 64, and slice thickness = 3.8 mm. The imaging protocol also included T_2-weighted structural images, which as noted previously were reviewed as part of the screening process, and DTI.

The DTI sequence included 30 near-axial slices, parallel to AC-PC, with no interslice gap. Data were acquired with six directions of diffusion sensitizing gradients, plus an image data set without diffusion weighting. DTI scan parameters included TR/TE = 30000/138.8, b = 1000 sec/mm^2, NEX = 1, in-plane resolution = 1.875 mm, flip angle = 90°, FOV = 24 cm, image matrix = 128 × 128, and slice thickness = 3.8 mm. Mean fractional anisotropy (FA) was extracted from seven ROIs, defined in native space on the DTI images for each participant (Bucur et al. 2008). These ROIs targeted the uncinate fasciculus, the genu and splenium of the corpus callosum, a pericallosal frontal region, the cingulum bundle, and anterior and posterior portions of the superior longitudinal fasciculus (Figure 3). FA is a scalar value between 0 and 1.0 that represents the directionality of the diffusion of molecular water (Basser & Jones 2002, Beaulieu 2002). Decreases in FA occur as the result many factors including a reduction in myelination, and FA is used frequently as an index of age-related changes in cerebral white matter integrity (Sullivan & Pfefferbaum 2006, Madden et al. 2009a).

Connectivity Analyses

The developed BBCA method consists of two major steps. Step 1: The acquired fMRI data were low-pass filtered to suppress the task-evoked signal changes. The low-frequency fluctuations of the filtered signals, similar to data acquired in resting-state, reflect mainly the spontaneous brain activity. Step 2: The filtered fMRI data were then further processed with a new functional connectivity (FC) analysis to identify major behaviorally-relevant functional networks. These two steps are described below.

Step 1: Suppression of Task-Related BOLD Signal Changes—First, the acquired fMRI data were aligned to the first image in the time-series, to correct for subtle movement. A data set with excessive movement was identified and excluded from further analysis. Second, the aligned time-series data were low-pass filtered (cutoff: 0.1Hz) to suppress task evoked BOLD signal changes (> 0.28 Hz). The linear drift of time-series signals was also corrected on a pixel-by-pixel basis. Third, the filtered images were smoothed (with a 6 mm × 6 mm × 6mm full-width-at-half-maximum Gaussian kernel) and normalized to the Montreal Neurological Institute (MNI) coordinates. The output of Step 1 was a set of filtered and normalized images, similar to data acquired during the resting-state, revealing the spontaneous BOLD signal fluctuations.

Step 2: Functional Connectivity (FC) Analysis—The filtered data generated from Step 1 were further processed with a new FC analysis method consisting of the following procedures.

A. fMRI data were segmented into 116 ROIs, using the Automated Anatomical Labeling (AAL) template created by Tzourio-Mazoyer et al. (2002). Because our normalized images and the AAL template are both in MNI coordinates, the existing anatomical labels provided by the AAL template were directly applied to our normalized data after matching the coordinates.

B. The time-series signals within each ROI were averaged, so that the 4D fMRI data set (x, y, z, time point) was reduced to a 2D data set (116 × time point number) for each fMRI run.

C. The correlation coefficients (*r* values) between time-series data from different anatomical regions were calculated, and the calculated coefficients (Fisher *z*-transformed) were stored in a 2D matrix with 6670 cells (i.e., 116 × 116, with only 116 × 115 / 2 unique elements; Figure 4a). Each element of this 2D matrix represents FC between two anatomical regions (Liu et al. 2007). This procedure was performed for all fMRI runs acquired from younger and older adults. This procedure corresponds to Figure 1-c1.

D. To identify the inter-region connectivity that is relevant to behavioral performance, the 2D matrix data from all participants within each age group were correlated with mean RT in the choice RT task (Figure 1-c2). That is, within each age group, a correlation was calculated (across participants) between the Fisher *z* value of each matrix cell and mean choice RT. This correlation was conducted at each of the 6670 cells of the matrix. For each age group, behaviorally-relevant functional networks were then identified by thresholding these correlations at $p < .005$ (uncorrected).

E. The identified behaviorally-relevant functional networks (from the preceding step) were then validated with an independent analysis, which compared the FC values for younger and older adults and evaluated the relation between FC and choice RT within each age group.

Because the developed data processing method directly compared data across participants, it is important to ensure that the data sets were properly normalized to the chosen AAL template. We have implemented a mask-based, quality-control procedure to detect inaccurate image normalization, for each of the 116 anatomical regions defined in AAL template. First, for each participant, an image mask was created for each anatomical region of normalized fMRI data, by assigning 1 to voxels with significant signal intensities (i.e., 10% of the maximal signal intensity measured from the whole brain) and 0 to remaining voxels. Second, by comparing the created mask with the original AAL template on a region-by-region basis, improper image normalization, in any anatomical region, could be identified for each participant. Specifically, we calculated the ratio of unmatched voxel number to the total voxel number in each AAL-defined region (between 0 and 100%), as our region-based inaccuracy index. The region-based normalization accuracy index was then defined as 1 minus the inaccuracy index.

Results

Identification of Functionally Connected Regions

An example of a 116 × 116 inter-region connectivity matrix is shown in Figure 4a, which is the average of connectivity matrices obtained from the 19 younger adults. As described in Step 2C in the Methods section, the grayscale value of each element of this 2D matrix represents the degree of signal coherence (i.e., the connectivity) between two brain regions. For example, the orange cluster in Figure 4a is a 2 × 2 set of four neighboring matrix cells, representing the connectivity between left / right medial-prefrontal cortex (shown in red) and left / right posterior cingulate (shown in yellow), as schematically illustrated in Figure 4b.

Analyses were conducted on the inter-region connectivity matrices in four sets of data, representing each combination of run type (semantic, episodic) and age group (younger, older). The semantic run for one younger adult was discarded due to excessive head motion, otherwise complete data were available for each participant, yielding a total of 75 fMRI runs: 19 episodic

runs for each age group, 19 semantic runs for older adults and 18 semantic runs for younger adults.

The task effect on the inter-region connectivity matrices was quantified by correlating each matrix element from all fMRI runs with a task category array, which was a 1 × 75 array with episodic versus semantic coded as 0 or 1. At a threshold of $p < .01$ (uncorrected), there was no significant difference in the inter-region connectivity matrices between semantic and episodic fMRI data. This result confirms that the task-associated functional activity was effectively suppressed, as intended in the data processing (Step 1).

Similarly, the age group effect on the inter-region connectivity matrices was quantified by correlating each connectivity matrix element from all fMRI runs with an age category array, which was a 1 × 75 array with age group coded as either 0 or 1. In this analysis, with the correlations thresholded at $p < .001$(uncorrected), 66 inter-region connectivity matrix elements were significantly lower for older adults than for younger adults. For example, the *Zr* values for the default mode network connectivity (i.e., between the medial-prefrontal cortex and the posterior cingulate, see Figure 4b) were 0.75±0.22 and 0.57±0.38, respectively, for younger and older adults. This observation agrees with previous reports on age-related reduction in the default mode network connectivity (Andrews-Hanna et al. 2007, Wu et al. 2007, Damoiseaux et al. 2008, Sambataro et al. 2008).

Identification of Behaviorally-Relevant Networks

To this point in the analyses, the relation between FC and behavioral performance has not been considered. In the next series of analyses, we examined the degree to which networks of connectivity were related to behavioral performance (specifically, choice RT) and whether this relation varied as a function of age group.

Because in the previous analyses, FC did not vary significantly as a function of task, the connectivity matrices derived from semantic and episodic fMRI runs were averaged for each participant, and these averaged matrices were used in subsequent analyses. We then obtained the correlation coefficients between each connectivity matrix element and choice RT for each participant. The mean choice RT values (averaged across all runs) were significantly higher for older adults ($M = 503$, $SD = 83$), than for younger adults ($M = 437$, $SD = 68$), $t(36) = 2.68$, $p < .01$, reflecting an age-related slowing in this task. At a threshold of $p < .005$ (uncorrected), none of the younger adults' connectivity matrix elements was significantly correlated with the choice RT. For older adults, however, 33 elements in the connectivity matrix were significantly correlated with the choice RT at this threshold (corresponding to $r = 0.615$). All of these correlations were negative, reflecting increased RT (slower responses) as a function of decreasing connectivity. The FC values for these 33 pairs of regions are presented in Table 1. Among those 33 pairs, 19 of them involve connections only within the cerebral areas, and 14 of them also involve connections to the cerebellum. We focused on only the connectivity within the cerebral areas, because the cerebellum was more susceptible to errors related to image normalization. Based on our mask-based quality-control procedure, the image normalization was highly accurate for cerebral regions (99.74%), and was less accurate for the cerebellum (91.82%).

Figure 5 shows those 19 behaviorally-relevant FC networks (red lines) for the older adults, as well as the anatomical regions connected by those networks (with AAL template labels). The majority of the behaviorally-relevant functional networks (i.e., 13 out of 19) were connected within or to the inferior frontal area (indicated by purple boxes with blue background in Figure 5).

Relation of Functional Connectivity to Age-Related Slowing

We next focused on the 13 pairs of regions involving the inferior frontal cortex, and examined the strength of the relation between FC and choice RT in these regions. We averaged the mean FC values across these 13 regions to obtain a single FC measure. This average FC did not differ significantly between younger adults (M = 0.843, SD = 0.227) and older adults (M = 0.898, SD = 0.259). A linear regression analysis of the FC values, using age group, choice RT, and their interaction as predictors, indicated that the predictors could account for 40% of the variance in FC, $F(3, 34) = 7.49$, $p < .001$. In this regression model, the Age Group × RT interaction term was significant, $t(34) = -3.05$, $p < .01$, indicating that the relation between RT and FC varied significantly across the age groups. As illustrated in Figure 6, this interaction occurred because the older adults exhibited a significant correlation between RT and FC, $r = -0.830$, $p < .0001$, whereas the younger adults exhibited no significant relation between these variables. That is, older adults exhibiting higher FC values responded more rapidly (lower RT) in the choice RT task.

Bivariate correlations (Table 2) indicated that, within the older adult group, there was a significant increase in RT as a function of increasing years of age ($p < .05$). That is, the age-related slowing of behavioral performance was detectable within in the older group, as well as between the two age groups. Increasing years of age, within the older adult group, was also associated with decreasing FC, and this correlation was near our significance threshold at $p < .06$. Neither of these effects approached significance within the younger adult group ($p > .25$ in each case).

We examined the degree to which the relation between years of age and RT, for older adults, was influenced by FC. Specifically, is the older adults' age-related slowing of behavioral performance mediated by FC? To investigate mediation we estimated the degree to which the older adults' age-related variance in RT was attenuated by statistically controlling the effect of FC (Salthouse 1992). These analyses are summarized in Table 3. When years of age was the sole predictor of the older adults' RT, this predictor accounted for 29% of the variance in older adults' RT. When, however, FC was entered into the regression model before age, then age only accounted for an additional 3.7% of the variance in RT. In other words, controlling for individual differences in FC attenuated the age-related variance in the older adults' RT by 87%. This result indicates that FC is a mediator of the age-related slowing in the older adults' behavioral performance.

Previous investigations of intrinsic FC that have incorporated DTI suggest that FC networks are related to the integrity of associated white matter pathways (van den Heuvel et al. 2008, Greicius et al. 2009). Given the role of FC as a mediator of older adults' behavioral performance, in the present data, we investigated whether cerebral white matter integrity, obtained from DTI, was a potential mechanism of individual differences in the older adults' FC values. Mean FA data from seven ROIs are presented in Table 4. These ROIs were selected to represent some of the major pathways connecting cortical regions that are critical for cognitive function (Bucur et al. 2008). In a regression model with FA from all seven regions included as seven predictors of FC, for older adults, only genu FA was a significant predictor, $t(11) = 2.34$, $p < .05$. The correlation between genu FA and FC was positive, $r = 0.535$, indicating that older adults with higher genu FA values exhibited higher mean FC, across the 13 regions associated with the inferior frontal gyri (Figure 7).

Discussion

In previous FC studies the main focus has primarily been on detecting differences of the functional connectivity strength between younger and older adults. In contrast, here we report a whole-brain analysis method to identify the FC networks that are best correlated with the

behavioral measures, independently of the connectivity level difference between age groups. Our method is similar to the previous approaches in that we suppress the task-evoked signal (using a low-pass, < 0.1 Hz filter) to extract the spontaneous, low-frequency fluctuations in the BOLD signal and then compute the correlation between the averaged time course data across brain regions. The new feature of our method is that no assumptions are required regarding the anatomical location of behaviorally-relevant regions. All pairwise correlations among 116 regions in a standardized template (Tzourio-Mazoyer et al. 2002) are examined in parallel. In addition, in contrast to seed-based or ICA-based approaches, the behavioral data are incorporated in an earlier stage of processing and contribute directly to defining the FC networks (Figure 1).

In applying the BBCA method to fMRI data of healthy, younger and older adults, we obtained three main findings that support our initial hypotheses. First, significant age-related change was evident in the behaviorally-relevant FC networks. Second, our method identified behaviorally-relevant, intrinsic FC outside of the default mode network. Third, intrinsic FC was related to structural connectivity as reflected in cerebral white matter integrity. In the following discussion, we briefly note some of the implications of these three findings.

Adult Age Differences in Functional Connectivity

Arguably the most important of the present findings is the difference between younger and older adults in the relation between the magnitude of FC and elementary perceptual-motor speed (Figure 6). In this analysis, we selected the 13 FC networks that involved the inferior frontal gyri and found that, within the combined data for all participants, the relation between the averaged FC in these regions and choice RT differed significantly across the age groups. Older adults exhibited a highly linear relation (r = -0.830) between increasing connectivity and decreasing RT (i.e., faster responses), whereas no relation between these variables was evident for younger adults. Further analyses, conducted within the older adult group, demonstrated that choice RT increased significantly as a function of increasing years of age, and that mean FC was a mediator of the older adults' age-related slowing. When the relation between older adults' years of age and RT was controlled statistically for individual differences in FC, the age-related variance in RT was attenuated by 87% (Table 3). Although there are no established guidelines for interpreting the magnitude of statistical attenuation, Salthouse (1992) proposed that attenuation effects of 60% or more represent major influences. Elementary perceptual-motor speed is well established as a fundamental component of cognitive aging, which shares age-related variance with a wide variety of cognitive measures (Salthouse 1996,Madden 2001,Salthouse & Madden 2007). The present results suggest that the coherence of spontaneous, low-frequency fluctuations in brain activity, involving the inferior frontal cortex, may be a mechanism of age-related cognitive slowing.

The correlation between FC and RT, for older adults (Figure 6), is broadly consistent with previous investigations reporting that older adults' decreased FC is associated with decreasing performance on various cognitive measures (Andrews-Hanna et al. 2007,Wu et al. 2007,Damoiseaux et al. 2008,Sambataro et al. 2008). The present findings, however, differ critically from the previous results. The previous studies did not specifically examine the degree to which age-related variance in cognitive performance was shared with FC. The present analyses demonstrated that the age-dependent increase in choice RT, for older adults, was nearly entirely (87%) shared with individual differences in FC. In addition, as discussed in the following section, the earlier investigations (with the exception of Wu et al. (2007) focused almost exclusively on brain regions typically defined as comprising the default mode network, whereas our FC regions are distributed widely outside of that network.

Distributed Behaviorally-Relevant Networks

The FC networks exhibiting a significant relation to choice RT were distributed widely, beyond the typical components of the default mode network (e.g., medial prefrontal and posterior cingulate cortex). Our method identified 19 pairs of connected regions in the superior, medial and inferior frontal gyri, anterior cingulate, insula, occipital cortex, thalamus, and several regions in the temporal lobe (Table 1). The majority of the networks (13), however, involved either the left or right inferior frontal gyrus, suggesting that these latter regions are of particular importance, in relation to perceptual-motor speed (Figure 5). Various types of cognitive processes have been associated with inferior frontal cortex, and on the basis of the present data it is not possible to determine the exact nature of the cognitive demands that are relevant for intrinsic FC in this region. Studies of task-related activation frequently conclude that inferior frontal activation in the left hemisphere represents the retrieval of semantic information (Demb et al. 1995,Fiez 1997), whereas right inferior frontal activation represents the inhibitory control of motor responses (Garavan et al. 1999,Konishi et al. 1999). Thompson-Shill et al. (1997), however, proposed that left inferior frontal activation represents the selection among competing alternatives rather than semantic retrieval *per se*. This more elementary process of response selection accords with related findings, from both lesion and task-related activation studies, suggesting that the left inferior frontal gyrus is significantly involved with attention and inhibitory control (Brass & von Cramon 2004,Swick et al. 2008). The present results indicate that a relation between inferior frontal activity and the selection of a motor response (choice RT) is not limited to event-related activation, but it also evident in the spontaneous, low-frequency fluctuations in the BOLD signal.

The behaviorally-relevant FC networks illustrated in Figure 5 were significant only for older adults. We chose a relatively conservative threshold of $p < .005$ (corresponding to $r = 0.615$), to restrict the number of networks identified for the older adults, while maintaining the same threshold for both age groups. To identify FC networks for younger adults, using this method, it may be necessary to a more liberal statistical threshold for the FC-behavior correlation. The sensitivity of this method is also likely influenced by the variability of the behavioral measure and the size of the ROIs used for correlation. That is, by using a behavioral measure yielding a wider range of performance values, or using ROIs that are smaller in size (i.e., more regionally specific), we may be more successful in identifying behaviorally-relevant FC for younger adults.

White Matter Integrity and Functional Connectivity

Analysis of cerebral white matter integrity, indexed by FA from DTI, revealed a significant relation between white matter integrity and older adults' mean FC. With other regional measures of FA covaried, only FA in the genu exhibited a positive correlation with FC: Those older adults with higher white matter integrity were those with higher values of mean FC across the regions connecting to the inferior frontal gyri. In our previous analyses of the behavioral and DTI data from this study, we found that cerebral white matter integrity, particularly within the genu and pericallosal frontal regions, was a mediator of the relation between perceptual-motor speed (choice RT) and episodic memory retrieval (Bucur et al. 2008). The present analysis extends these previous findings by demonstrating that, within the older adults' data, white matter integrity is associated with FC, which in turn mediates age-related slowing.

The correlation between the older adults' genu FA and mean FC is consistent with other investigations, using DTI, which have demonstrated a relation between white matter integrity and intrinsic FC. In studies of younger adults, van den Heuvel et al. (2008) demonstrated a positive correlation between FA in the cingulum bundle and FC, and Greicius et al. (2009) reported that the regional distribution of the FC map was consistent with DTI tractography. Andrews-Hanna et al. (2007) found that older adults' mean FA from a large ROI (centrum

semiovale) correlated positively with FC. These previous studies focused primarily on regions in the default mode network. Our finding that only FA in the genu was correlated significantly with the older adults' FC values (Figure 7) is intriguing in that the genu provides the interhemispheric connections for the frontal lobe, and our behaviorally-relevant measure of FC is comprised primarily of connections through the inferior frontal gyri (Figure 5). More generally, the relation between white matter integrity and FC supports a disconnection model of neurocognitive aging, in which age-related changes in cognitive performance represent the interaction of structural and functional connectivity across distributed neural systems (Bartzokis et al. 2004, Andrews-Hanna et al. 2007, Sullivan et al. 2008, Davis et al.2009, Madden et al. 2009b).

Limitations

There are several limitations to the present research, related to both the measurement of FC and the analysis of adult age differences. As noted previously in this Discussion, although our method does not require *a priori* assumptions regarding the location of the relevant brain regions, the anatomical template (Tzourio-Mazoyer et al. 2002) may not be as sensitive as a voxelwise approach for detecting FC, particularly when the voxel-wise connectivity levels within an anatomical region are not homogeneous. In addition, the present sample size, 19 participants in each of two age groups, limits the statistical power to detect both regional FC and age-related change. Our measure of behaviorally-relevant FC averages across 13 pairs of regions involving the inferior frontal gyri, and we have not yet identified the relative contributions of individual networks to this composite measure. Our conclusions regarding white matter integrity are based on relatively low-resolution, non-isotropic DTI data. Ideally, further research can include a larger sample size and multiple measures of cognition, FC, and white matter integrity, in a longitudinal design, to estimate the relative influence of structural and functional connectivity in age-related cognitive change (Raz et al. 2005, Raz et al. 2007).

In our study, the stimuli were presented at three frequency values: 0.285, 0.333, and 0.4 Hz. Therefore, the low-pass filtering (<0.1 Hz) can eliminate the task evoked responses. Our data showed that the intrinsic connectivity networks derived from two different task conditions (episodic-memory and semantic-memory) are statistically the same, indicating that the task evoked responses have been effectively suppressed in the post-processing. In general, the task and stimuli (of high temporal-frequency) may possibly alter the underlying intrinsic neuronal connectivity (of low temporal-frequency: <0.1 Hz), and thus the intrinsic connectivity networks derived from task-fMRI data (as in our study) and task-free resting-state fMRI data may not be identical. The potential difference between intrinsic connectivity networks in non-resting-state and task-free resting-state is not a concern in our study (for comparing neuronal networks between age groups), because we use identical acquisition and data processing methods for younger and older participants.

Conclusion

We have demonstrated a data processing approach for identifying age group differences in behaviorally-relevant, intrinsic FC, independently of age group differences in functional connectivity strength. Further, this whole-brain, voxelwise approach does not depend on defining ROIs in advance. Our results indicate that healthy, younger and older adults differ significantly in behaviorally-relevant FC. Older adults exhibited a significant relation between perceptual-motor speed (choice RT) and FC across a distributed network of brain regions involving the inferior frontal gyri, whereas no relation between behavior and FC was evident for younger adults. In addition, within the older adult group, the age-related variance in perceptual-motor speed was shared nearly entirely with FC, suggesting that intrinsic FC is a potential mechanism of age-related cognitive slowing. White matter integrity within the genu of the corpus callosum was correlated with older adults' FC. Combining the perspectives from

analyses of behaviorally-relevant FC, white matter integrity, and behavioral measures can contribute to a more complete account of age-related changes in cognitive performance.

Acknowledgments

This research was supported by research grants R01 AG011622 (DJM) and R01 NS050329 (AWS) from the National Institutes of Health.

References

Andrews-Hanna JR, Snyder AZ, Vincent JL, Lustig C, Head D, Raichle ME, Buckner RL. Disruption of large-scale brain systems in advanced aging. Neuron 2007;56:924–935. [PubMed: 18054866]

Basser PJ, Jones DK. Diffusion-tensor MRI: theory, experimental design and data analysis - a technical review. NMR Biomed 2002;15:456–467. [PubMed: 12489095]

Beaulieu C. The basis of anisotropic water diffusion in the nervous system - a technical review. NMR Biomed 2002;15:435–455. [PubMed: 12489094]

Beck, AT. The Beck depression inventory. Psychological Corporation; New York: 1978.

Binder JR, Frost JA, Hammeke TA, Bellgowan PS, Rao SM, Cox RW. Conceptual processing during the conscious resting state. A functional MRI study. J Cogn Neurosci 1999;11:80–95. [PubMed: 9950716]

Biswal B, Yetkin FZ, Haughton VM, Hyde JS. Functional connectivity in the motor cortex of resting human brain using echo-planar MRI. Magn Reson Med 1995;34:537–541. [PubMed: 8524021]

Brass M, von Cramon DY. Decomposing components of task preparation with functional magnetic resonance imaging. J Cogn Neurosci 2004;16:609–620. [PubMed: 15165351]

Bucur B, Madden DJ, Spaniol J, Provenzale JM, Cabeza R, White LE, Huettel SA. Age-related slowing of memory retrieval: contributions of perceptual speed and cerebral white matter integrity. Neurobiol Aging 2008;29:1070–1079. [PubMed: 17383774]

Christensen KJ, Moye J, Armson RR, Kern TM. Health screening and random recruitment for cognitive aging research. Psychol Aging 1992;7:204–208. [PubMed: 1610509]

Damoiseaux JS, Beckmann CF, Arigita EJ, Barkhof F, Scheltens P, Stam CJ, Smith SM, Rombouts SA. Reduced resting-state brain activity in the “default network” in normal aging. Cereb Cortex 2008;18:1856–1864. [PubMed: 18063564]

Damoiseaux JS, Rombouts SA, Barkhof F, Scheltens P, Stam CJ, Smith SM, Beckmann CF. Consistent resting-state networks across healthy subjects. Proc Natl Acad Sci U S A 2006;103:13848–13853. [PubMed: 16945915]

Davis SW, Dennis NA, Buchler NG, White LE, Madden DJ, Cabeza R. Assessing the effects of age on long white matter tracts using diffusion tensor tractography. Neuroimage 2009;46:530–541. [PubMed: 19385018]

De Luca M, Beckmann CF, De Stefano N, Matthews PM, Smith SM. fMRI resting state networks define distinct modes of long-distance interactions in the human brain. Neuroimage 2006;29:1359–1367. [PubMed: 16260155]

Demb JB, Desmond JE, Wagner AD, Vaidya CJ, Glover GH, Gabrieli JD. Semantic encoding and retrieval in the left inferior prefrontal cortex: a functional MRI study of task difficulty and process specificity. J Neurosci 1995;15:5870–5878. [PubMed: 7666172]

Dennis, NA.; Cabeza, R. Neuroimaging of healthy cognitive aging. In: Craik, FIM.; Salthouse, TA., editors. The handbook of aging and cognition. Psychology Press; New York: 2008. p. 1-54.

Fair DA, Schlaggar BL, Cohen AL, Miezin FM, Dosenbach NU, Wenger KK, Fox MD, Snyder AZ, Raichle ME, Petersen SE. A method for using blocked and event-related fMRI data to study “resting state” functional connectivity. Neuroimage 2007;35:396–405. [PubMed: 17239622]

Fiez JA. Phonology, semantics, and the role of the left inferior prefrontal cortex. Hum Brain Mapp 1997;5:79–83. [PubMed: 10096412]

Folstein MF, Folstein SE, McHugh PR. “Mini-mental state”. A practical method for grading the cognitive state of patients for the clinician. J Psychiatr Res 1975;12:189–198. [PubMed: 1202204]

Fox MD, Corbetta M, Snyder AZ, Vincent JL, Raichle ME. Spontaneous neuronal activity distinguishes human dorsal and ventral attention systems. Proc Natl Acad Sci U S A 2006;103:10046–10051. [PubMed: 16788060]

Fox MD, Snyder AZ, Vincent JL, Corbetta M, Van Essen DC, Raichle ME. The human brain is intrinsically organized into dynamic, anticorrelated functional networks. Proc Natl Acad Sci U S A 2005;102:9673–9678. [PubMed: 15976020]

Fox MD, Snyder AZ, Vincent JL, Raichle ME. Intrinsic fluctuations within cortical systems account for intertrial variability in human behavior. Neuron 2007;56:171–184. [PubMed: 17920023]

Garavan H, Ross TJ, Stein EA. Right hemispheric dominance of inhibitory control: an event-related functional MRI study. Proc Natl Acad Sci U S A 1999;96:8301–8306. [PubMed: 10393989]

Grady CL. Cognitive neuroscience of aging. Ann N Y Acad Sci 2008;1124:127–144. [PubMed: 18400928]

Greicius MD, Krasnow B, Reiss AL, Menon V. Functional connectivity in the resting brain: a network analysis of the default mode hypothesis. Proc Natl Acad Sci U S A 2003;100:253–258. [PubMed: 12506194]

Greicius MD, Srivastava G, Reiss AL, Menon V. Default-mode network activity distinguishes Alzheimer's disease from healthy aging: evidence from functional MRI. Proc Natl Acad Sci U S A 2004;101:4637–4642. [PubMed: 15070770]

Greicius MD, Supekar K, Menon V, Dougherty RF. Resting-state functional connectivity reflects structural connectivity in the default mode network. Cereb Cortex 2009;19:72–78. [PubMed: 18403396]

Hampson M, Peterson BS, Skudlarski P, Gatenby JC, Gore JC. Detection of functional connectivity using temporal correlations in MR images. Hum Brain Mapp 2002;15:247–262. [PubMed: 11835612]

Konishi S, Nakajima K, Uchida I, Kikyo H, Kameyama M, Miyashita Y. Common inhibitory mechanism in human inferior prefrontal cortex revealed by event-related functional MRI. Brain 1999;122:981–991. [PubMed: 10355680]

Kučera, H.; Francis, WN. Computational analysis of present-day American English. Brown University Press; Providence, RI: 1967.

Lustig C, Snyder AZ, Bhakta M, O'Brien KC, McAvoy M, Raichle ME, Morris JC, Buckner RL. Functional deactivations: change with age and dementia of the Alzheimer type. Proc Natl Acad Sci U S A 2003;100:14504–14509. [PubMed: 14608034]

Madden, DJ. Speed and timing of behavioral processes. In: Birren, JE.; Schaie, KW., editors. Handbook of the psychology of aging. Academic Press; San Diego, CA: 2001. p. 288-312.

Madden DJ, Bennett IJ, Song AW. Cerebral white matter integrity and cognitive aging: Contributions from diffusion tensor imaging. Neuropsych Rev. 2009a

Madden DJ, Spaniol J, Costello MC, Bucur B, White LE, Cabeza R, Davis SW, Dennis NA, Provenzale JM, Huettel SA. Cerebral white matter integrity mediates adult age differences in cognitive performance. J Cogn Neurosci 2009b;21:289–302. [PubMed: 18564054]

Mazoyer B, Zago L, Mellet E, Bricogne S, Etard O, Houde O, Crivello F, Joliot M, Petit L, Tzourio-Mazoyer N. Cortical networks for working memory and executive functions sustain the conscious resting state in man. Brain Res Bull 2001;54:287–298. [PubMed: 11287133]

Persson J, Lustig C, Nelson JK, Reuter-Lorenz PA. Age differences in deactivation: a link to cognitive control? J Cogn Neurosci 2007;19:1021–1032. [PubMed: 17536972]

Raichle ME, MacLeod AM, Snyder AZ, Powers WJ, Gusnard DA, Shulman GL. A default mode of brain function. Proc Natl Acad Sci U S A 2001;98:676–682. [PubMed: 11209064]

Raz N, Lindenberger U, Rodrigue KM, Kennedy KM, Head D, Williamson A, Dahle C, Gerstorf D, Acker JD. Regional brain changes in aging healthy adults: general trends, individual differences and modifiers. Cereb Cortex 2005;15:1676–1689. [PubMed: 15703252]

Raz N, Rodrigue KM, Kennedy KM, Acker JD. Vascular health and longitudinal changes in brain and cognition in middle-aged and older adults. Neuropsychology 2007;21:149–157. [PubMed: 17402815]

Salthouse, TA. Mechanisms of age-cognition relations in adulthood. Erlbaum, Hillsdale; NJ: 1992.

Salthouse TA. The processing-speed theory of adult age differences in cognition. Psychol Rev 1996;103:403–428. [PubMed: 8759042]

Salthouse, TA.; Madden, DJ. Information processing speed and aging. In: Deluca, J.; Kalmar, J., editors. Information processing speed in clinical populations. Psychology Press; New York: 2007. p. 221-241.

Sambataro F, Murty VP, Callicott JH, Tan HY, Das S, Weinberger DR, Mattay VS. Age-related alterations in default mode network: Impact on working memory performance. Neurobiol Aging. 2008

Seeley WW, Menon V, Schatzberg AF, Keller J, Glover GH, Kenna H, Reiss AL, Greicius MD. Dissociable intrinsic connectivity networks for salience processing and executive control. J Neurosci 2007;27:2349–2356. [PubMed: 17329432]

Shulman GL, Fiez JA, Corbetta M, Buckner RL, Miezin FM, Raichle ME, Petersen SE. Common blood flow changes across visual tasks: II. Decreases in cerebral cortex. Journal of Cognitive Neuroscience 1997;9:648–663.

Smith SM, Jenkinson M, Johansen-Berg H, Rueckert D, Nichols TE, Mackay CE, Watkins KE, Ciccarelli O, Cader MZ, Matthews PM, Behrens TE. Tract-based spatial statistics: voxelwise analysis of multi-subject diffusion data. Neuroimage 2006;31:1487–505. [PubMed: 16624579]

Sullivan EV, Pfefferbaum A. Diffusion tensor imaging and aging. Neurosci Biobehav Rev 2006;30:749–761. [PubMed: 16887187]

Swick D, Ashley V, Turken AU. Left inferior frontal gyrus is critical for response inhibition. BMC Neurosci 2008;9:102. [PubMed: 18939997]

Thompson-Schill SL, D'Esposito M, Aguirre GK, Farah MJ. Role of left inferior prefrontal cortex in retrieval of semantic knowledge: a reevaluation. Proc Natl Acad Sci U S A 1997;94:14792–14797. [PubMed: 9405692]

Tzourio-Mazoyer N, Landeau B, Papathanassiou D, Crivello F, Etard O, Delcroix N, Mazoyer B, Joliot M. Automated anatomical labeling of activations in SPM using a macroscopic anatomical parcellation of the MNI MRI single-subject brain. Neuroimage 2002;15:273–289. [PubMed: 11771995]

van den Heuvel M, Mandl R, Luigjes J, Hulshoff Pol H. Microstructural organization of the cingulum tract and the level of default mode functional connectivity. J Neurosci 2008;28:10844–10851. [PubMed: 18945892]

Wechsler, D. Wechsler adult intelligence scale-revised, Vol. Psychological Corporation; New York: 1981.

Wu T, Zang Y, Wang L, Long X, Hallett M, Chen Y, Li K, Chan P. Aging influence on functional connectivity of the motor network in the resting state. Neurosci Lett 2007;422:164–168. [PubMed: 17611031]

Xiong J, Parsons LM, Gao JH, Fox PT. Interregional connectivity to primary motor cortex revealed using MRI resting state images. Hum Brain Mapp 1999;8:151–156. [PubMed: 10524607]

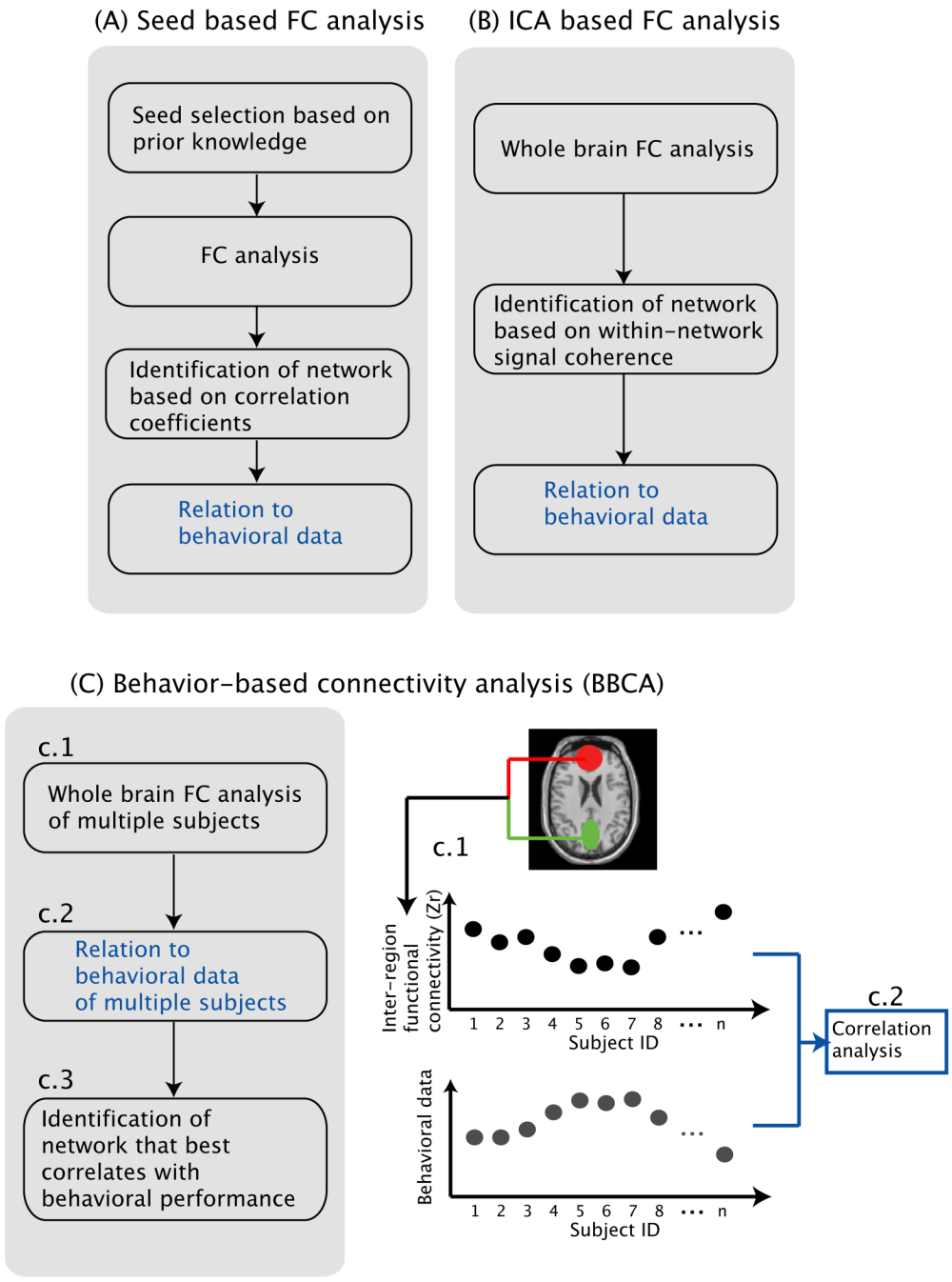

Fig 1.

Comparison of different approaches for calculating the relation between intrinsic functional connectivity (FC) and behavioral performance: seed-based region of interest (ROI; Panel A), independent components analysis (ICA; Panel B), and the BBCA method (Panel C). In comparison to conventional approaches (A and B), the BBCA method (C) integrates behavioral data at an early stage of processing, and evaluates the behavioral relevance of all intrinsic connectivity networks without a priori assumptions regarding the relevant regions. An FC matrix of all possible pairwise comparisons is first calculated for each subject (Panel C.1). By correlating the FC measures with the behavioral data across subjects (Panel C.2), the behaviorally-relevant FC can be identified with a pre-defined threshold (Panel C.3)

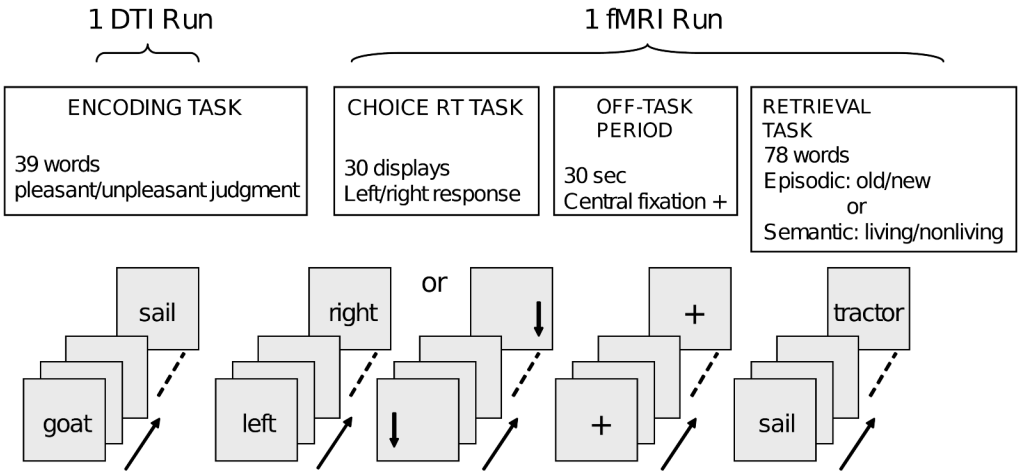

Fig 2.

Events occurring within each imaging run. Participants first performed a word encoding task (pleasant/unpleasant judgment of individual words) during diffusion tensor imaging (DTI). During a following functional magnetic resonance imaging (fMRI) run, participants performed a choice reaction time (RT) task (left/right key press), followed by an off-task period, and a memory retrieval task. The nature of the retrieval task, episodic versus semantic, alternated across runs. The episodic task required a yes/no judgment as to whether the current word was presented during encoding. The semantic task required a living/nonliving judgment regarding the referent of the word, without reference to the word's presence in the encoding list

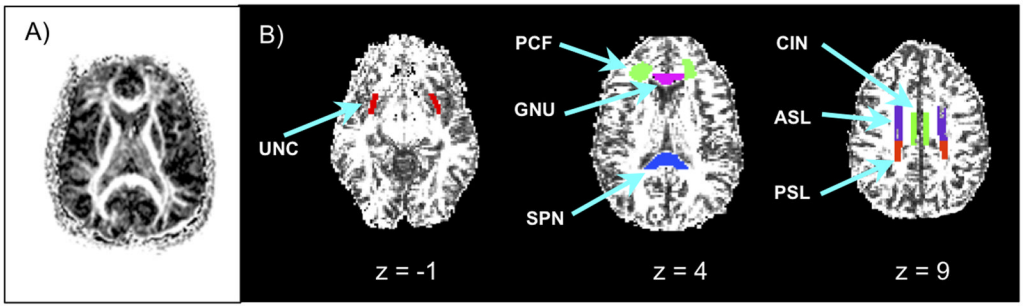

Fig 3.

Examples of the regions of interest ROIs used in the analysis of the diffusion tensor imaging (DTI) data, modified from Bucur et al. (2008). Panel A = raw DTI image. Panel B = regions located on DTI images with maximum value for image intensity lowered. UNC = uncinate fasciculus; PCF = pericallosal frontal; GNU = genu of corpus callosum; SPN = splenium of corpus callosum; CIN = cingulum bundle; ASL = anterior portion of the superior longitudinal fasciculus; PSL = posterior portion of the superior longitudinal fasciculus. The z values are mm superior/inferior to the anterior commissure

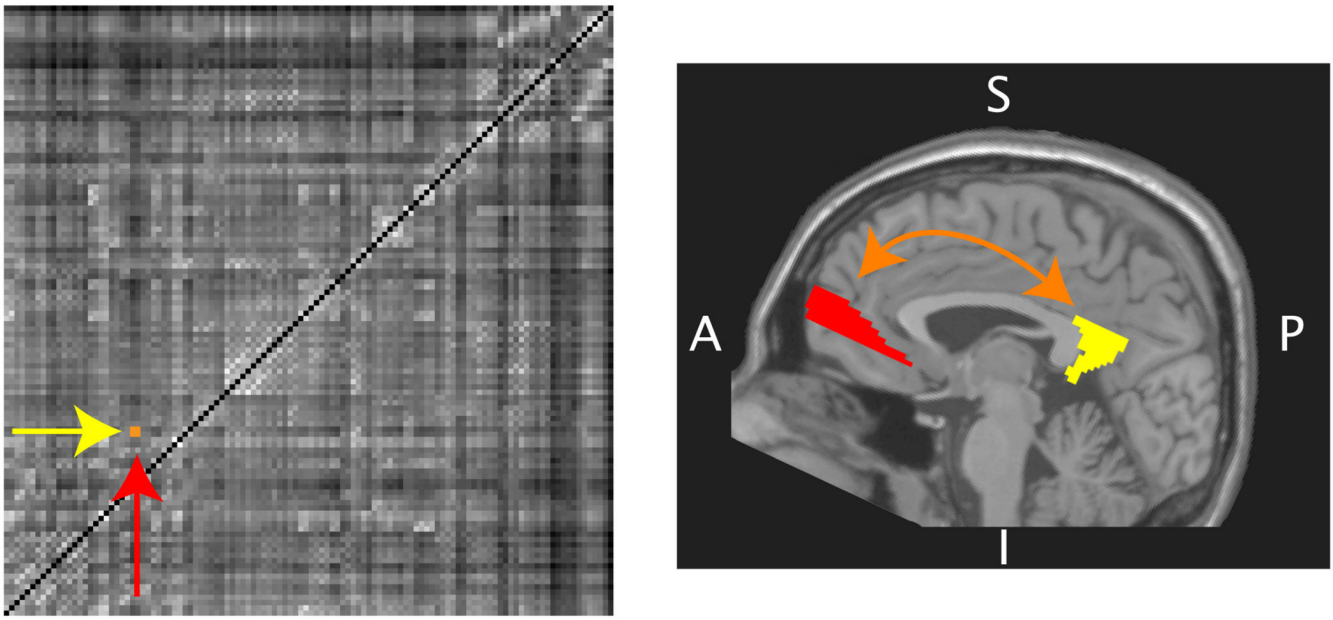

Fig 4.

Regional connectivity matrix for the 116 anatomical regions in the Tzourio-Mazoyer (2002) template. Within each cell of the matrix, the grayscale value represents the signal coherence level (*Zr*) between two regions (Panel A). For example, A 2 × 2 orange cluster (consisting of four neighboring matrix cells) represents the signal coherence levels between left/right medial prefrontal cortex (orbital; illustrated by red arrow) and left/right posterior cingulate (illustrated by yellow arrow). Panel B illustrates the location of medial prefrontal cortex (orbital) and posterior cingulate in a sagittal view

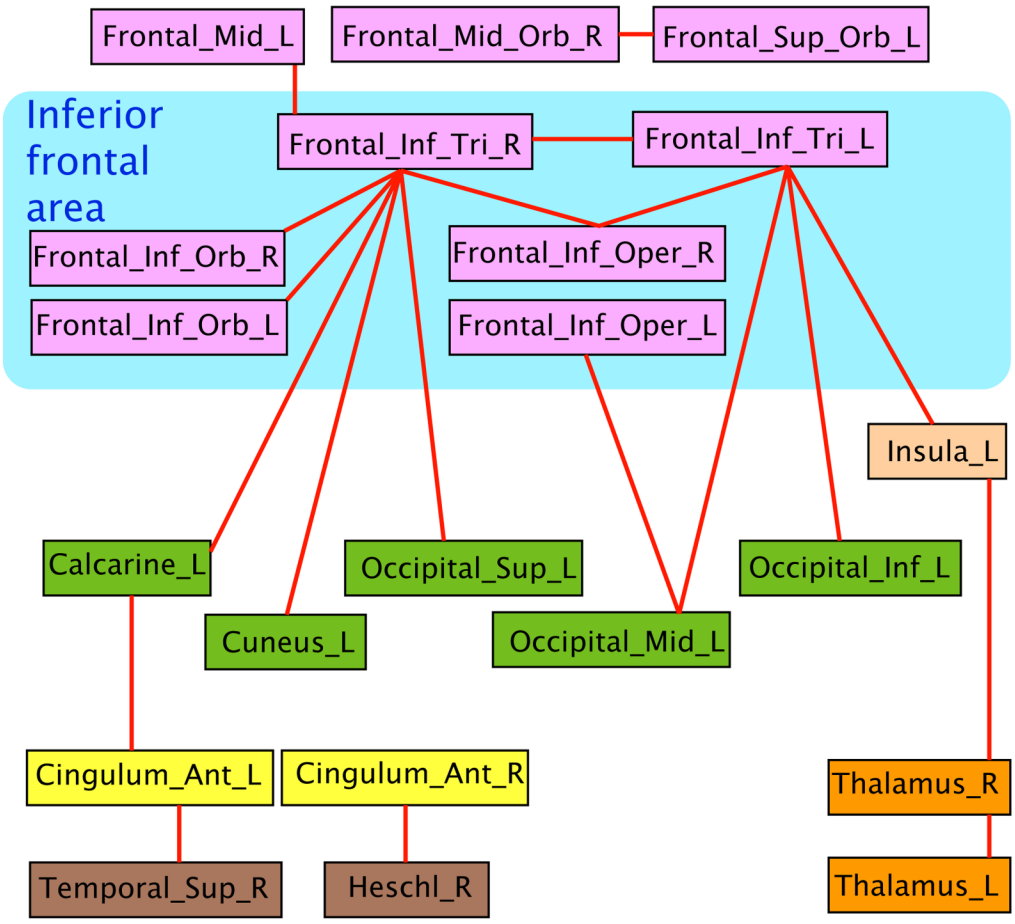

Fig 5.

In the regional connectivity matrix for older adults, 19 pairs of regions (indicated by red lines) were correlated significantly ($p < 0.005$) with perceptual-motor speed (choice reaction time; RT). The inferior frontal gyri were involved in 13 of these networks, indicating a role of the inferior frontal cortex in behaviorally-relevant functional connectivity (FC) for older adults. No regional connections were significant for younger adults at this threshold. For description of abbreviations, see Table 1 note

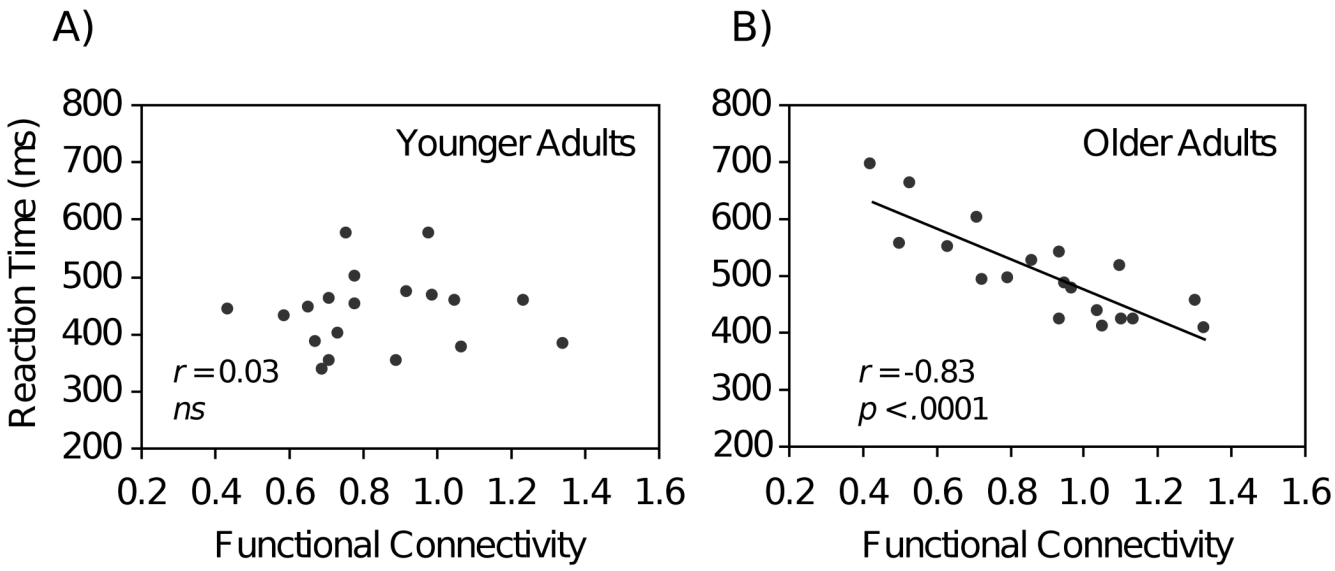

Fig 6.
Relation between choice reaction time (RT) and functional connectivity (in networks connected with inferior frontal gyri), for younger adults (Panel A) and older adults (Panel B)

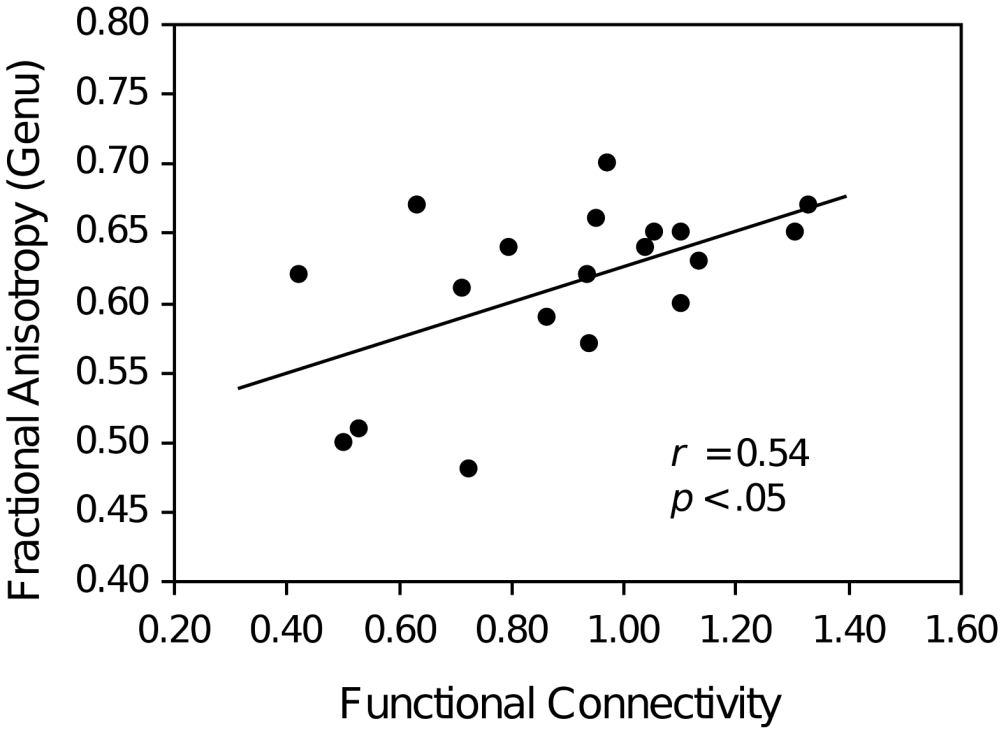

Fig 7.
Relation between white matter integrity (fractional anisotropy) in the genu of the corpus callosum and functional connectivity (in networks connected with inferior frontal gyri), for older adults

Brain Struct Funct. Author manuscript; available in PMC 2010 January 30.

Table 1

Functional Connectivity between Regions by Age Group

		M		*SD*	
Region 1	**Region 2**	**Younger**	**Older**	**Younger**	**Older**
Cerebral Connectivity					
Frontal_Sup_Orb_L	Frontal_Mid_Orb_R	0.915	0.851	0.338	0.252
Frontal_Mid_L	Frontal_Inf_Tri_R	0.679	0.839	0.388	0.352
Frontal_Inf_Oper_L	Occipital_Inf_L	0.772	0.773	0.251	0.276
Frontal_Inf_Oper_R	Frontal_Inf_Tri_L	0.853	0.941	0.357	0.283
Frontal_Inf_Oper_R	Frontal_Inf_Tri_R	1.362	1.235	0.374	0.415
Frontal_Inf_Tri_L	Frontal_Inf_Tri_R	0.733	0.813	0.436	0.394
Frontal_Inf_Tri_L	Insula_L	0.972	0.900	0.423	0.356
Frontal_Inf_Tri_L	Occipital_Mid_L	0.819	0.875	0.302	0.296
Frontal_Inf_Tri_L	Occipital_Inf_L	0.826	0.743	0.290	0.298
Frontal_Inf_Tri_R	Frontal_Inf_Orb_L	0.750	0.802	0.397	0.402
Frontal_Inf_Tri_R	Frontal_Inf_Orb_R	1.091	1.183	0.500	0.379
Frontal_Inf_Tri_R	Calcarine_L	0.634	0.765	0.273	0.232
Frontal_Inf_Tri_R	Cuneus_L	0.588	0.763	0.289	0.306
Frontal_Inf_Tri_R	Occipital_Sup_L	0.675	0.808	0.317	0.301
Insula_L	Thalamus_R	0.856	0.871	0.319	0.498
Cingulum_Ant_L	Cuneus_L	0.828	0.784	0.253	0.226
Cingulum_Ant_L	Temporal_Sup_R	0.742	0.819	0.248	0.300
Cingulum_Ant_R	Heschl_R	0.654	0.662	0.277	0.306
Thalamus_L	Thalamus_R	1.605	1.632	0.302	0.377
Cerebellar Connectivity					
Frontal_Sup_R	Cerebellum_Crus2_L	0.861	0.931	0.320	0.256
Frontal_Mid_L	Cerebellum_Crus1_L	0.860	0.902	0.227	0.220
Frontal_Mid_L	Cerebellum_Crus2_L	0.751	0.857	0.272	0.235
Frontal_Inf_Oper_L	Cerebellum_6_L	0.801	0.773	0.243	0.360

		M		*SD*	
Region 1	**Region 2**	**Younger**	**Older**	**Younger**	**Older**
Cerebral Connectivity					
Frontal_Inf_Oper_R	Cerebellum_Crus2_L	0.744	0.752	0.310	0.249
Frontal_Inf_Tri_L	Cerebellum_Crus1_L	0.774	0.743	0.288	0.262
Frontal_Inf_Tri_L	Cerebellum_Crus2_L	0.668	0.690	0.323	0.272
Frontal_Inf_Tri_L	Cerebellum_8_L	0.650	0.619	0.371	0.373
Frontal_Inf_Tri_R	Cerebellum_Crus1_L	0.721	0.718	0.249	0.260
Frontal_Inf_Tri_R	Cerebellum_Crus2_L	0.673	0.677	0.319	0.271
Frontal_Inf_Tri_R	Cerebellum_7b_L	0.463	0.547	0.413	0.272
Rectus_L	Cerebellum_Crus2_R	0.570	0.492	0.269	0.270
Insula_L	Cerebellum_4_5_L	0.690	0.737	0.305	0.356
Temporal_Pole_Sup_L	Cerebellum_10_R	0.462	0.411	0.298	0.239

Note. Functional connectivity (FC) values (Fisher *r* to *z* transform), calculated from younger and older groups, are listed only for those pairs of regions that exhibited a significant correlation ($p < .005$) with perceptual-motor speed (choice reaction time; RT) across older adults. No regions exceeded this threshold for younger adults; their values are listed for comparison.

Region 1 (or 2) = Regions that exhibited a significant correlation between FC and RT, for older adults. Labels for cerebral regions are from the Tzourio-Mazoyer (2002) template. Labels for cerebellar regions are from Schmahmann et al. (1999). Frontal_Sup_Orb_L = Left superior frontal gyrus, orbital part; Frontal_Mid_L = Left middle frontal gyrus; Frontal_Mid_Orb_R = Right middle frontal gyrus, orbital part; Frontal_Inf_Oper_L = Left inferior frontal gyrus, opercular part; Frontal_Inf_Oper_R = Right inferior frontal gyrus, opercular part; Frontal_Inf_Tri_L = Left inferior frontal gyrus, triangular part; Frontal_Inf_Tri_R = Right inferior frontal gyrus, triangular part; Frontal_Inf_Orb_L = Left inferior frontal gyrus, orbital part; Frontal_Inf_Orb_R = Right inferior frontal gyrus, orbital part; Insula_L = Left insula; Cingulum_Ant_L = Left anterior cingulate; Cingulum_Ant_R = Right anterior cingulate; Calcarine_L = Left calcarine fissure and surrounding cortex; Cuneus_L = Left cuneus; Occipital_Sup_L = Left superior occipital gyrus; Occipital_Mid_L = Left middle occipital gyrus; Occipital_Inf_L = Left inferior occipital gyrus; Thalamus_L = Left thalamus; Thalamus_R = Right thalamus; Heschl_R =Right heschl gyrus; Temporal_Sup_R = Right superior temporal gyrus; Rectus_L = Left gyrus rectus (Frontal lobe); Temporal_Pole_Sup_L = Left temporal pole, superior temporal gyrus (Limbic lobe); Frontal_Sup_R = Superior frontal gyrus, dorsolateral part.

Table 2
Correlation Between Variables by Age Group

	Younger		Older	
	RT	**Age**	**RT**	**Age**
Functional Connectivity	0.031	-0.042	-0.830**	-0.439
RT	--	-0.261	--	0.537*

Note. Values are Pearson *r*. Age = years; Functional Connectivity = mean connectivity for the 13 pairs of functionally correlated regions involving either the left or right inferior frontal gyrus (Figure 5); RT = mean choice reaction time.

* $p < .05$;

** $p < .0001$

Table 3

Mediation of Age-Related Slowing by Functional Connectivity

	B	*SE B*	r^2	Δr^2	*F*	Percentage Attenuation
Model 1						
Age	0.537	3.503	0.288		6.88*	
Model 2						
Functional Connectivity	-0.830	43.520	0.689		37.67***	
Age	0.214	2.493	0.726	0.037	2.16	87.15

Note. Data for older adults only (n = 19); dependent variable = choice reaction time; Age = years; Functional Connectivity = mean connectivity for the 13 pairs of functionally correlated regions involving either the left or right inferior frontal gyrus (Figure 5); *B* = standardized parameter estimate; *SE* = standard error; r^2 = cumulative r^2 for current and preceding steps; Δr^2 = unique effect of age.

* $p < .05$;

*** $p < .0001$

Table 4
Fractional Anisotropy by Age Group

	M		*SD*	
	Younger	**Older**	**Younger**	**Older**
Genu	0.655_a	0.614_b	0.017	0.060
Splenium	0.688_a	0.672_b	0.021	0.024
Pericallosal frontal	0.457_a	0.381_b	0.053	0.060
SLF anterior	0.457_a	0.415_b	0.043	0.046
SLF posterior	0.476_a	0.458_a	0.041	0.059
Uncinate fasciculus	0.536_a	0.525_a	0.068	0.060
Cingulum	0.505_a	0.445_b	0.055	0.053

Note. Values in the same row that do not share the same subscript differ at $p < .05$ (Bucur et al. 2008). SLF = superior longitudinal fasciculus.